Micro-Acoustic-Trap (μAT) for Microparticle Assembly in 3D

Varun Vyas[1(✉)], Michael Lemieux[3], David A. Knecht[3], Oleg Kolosov[2], Bryan D. Huey[1(✉)]

[1]Materials Science and Engineering Department, University of Connecticut, Storrs, CT 06269, United States

[2] Department of Physics, Lancaster University, Lancaster LA1 4YB, UK

[3]Department of Molecular and Cell Biology, University of Connecticut, Storrs, CT 06269, United States

ABSTRACT

With the current state of technology, use of Acoustic Tweezers (ATω) is limited to manipulation of single or few particles in single experimental setup. This article presents a state of the art system using Acoustic Lens (AL) as a Micro-Acoustic Trap (μAT) for microparticle assembly in 3D. In this investigation 2 micron sized polystyrene beads were used. Acoustic pressure generated by AL drives the particles towards the center of the acoustic focal plane, which leads to the formation of a free floating monolayer of latex particles. Transducer is driven at 89 MHz as both continuous wave (CW) and at mixed with pulsed (PL) frequency of 2Hz. The system was driven at drive amplitudes of 0.5 V, 1 V and 1.5 V. The most tightly packed monolayer of latex particles was observed at drive amplitude of 1.5 V. A loosely formed random close pack disc like structure was observed at 1 V whereas at 0.5 V drive amplitude particles were gently driven towards the center of the Acoustic Focal Plane (AFP) but no assemble was observed. This methodology was further extended for manipulating live *Dictyostelium discoideum* (Amoebas). At high drive amplitude of 2V, one can not only segregate non-adherent cells from adherent ones or move them to a region of interest but also can compress them and shrink their size. It was also observed that the cells having weaker cell membrane get distorted or membrane is rupture under a continuous stream of acoustic waves.

KEYWORDS

Micro-Acoustic-Trap (µAT) For Microparticle Assembly in 3D

Introduction

Micro to nanoscale events are constantly being explored and manipulated by means of both light and sound. It was with the discovery of radiation pressure exerted by a light source (focused laser) one could accelerate particles in the direction of light, thus lead to the development of optical tweezers (OTs)[1,2]. This enabled three dimensional trapping of particles and live cells such as E.coli for studying nanomechanical properties in an aqueous environment[3].

It was not until 90s acoustic tweezers (ATω) were developed by *Junru Wu*[4]. They were able to trap latex particles (270 µm) and a cluster of frog eggs in the potential well created by two opposing collimated focused ultrasonic beams in water. With recent developments in the design of acoustic transducers, researchers are able to perform contactless positioning and transport of matter in air[5] and liquid[6] environment. An ATω could be a simple acoustic lens (AL) [7]or a custom build heptagon acoustic tweezer for generating dynamic cell patterns at a user-determined position[8]. Holographic acoustic elements have recently gained lot of attention and are being used for levitating particles[9] and developing sound pressure images for contact less material handling and therapeutic applications of ultrasound[10].

Baresch *et al* has experimented with an AL to push and pull single polystyrene particle trapped in three dimensions[11]. Independent manipulation of multiple particles using a circular 64-element ultrasonic array brought dexterity of the ATω similar to that of OTs[12]. To improve imaging capabilities, ALs is being employed in number of biomedical investigations. Here a focused high-amplitude acoustic signal generated via an AL that uses nonlinear wave dynamic, creates a

transient focal region of higher energy density. This creates a compact acoustic pulse with higher accuracy and signal-to-noise ratios that can improve imaging capabilities as compared to currently available biomedical ultrasonic transducers[13]. Besides imaging other biomedical applications include bone repair using low intensity pulsed ultrasound (LIPUS)[14,15].

This article presents a unique application of AL were one can develop a Micro-Acoustic- Trap (μAT) to assemble monolayer of polystyrene microparticles/beads in 3D i.e. suspended in the bulk of the water. This assembled monolayer is similar to monolayer formed by polystyrene beads in nanosphere lithography (NSL)[16,17]. NSL involves drop coating of particle concentrate over spinning a glass coverslip. This spinning of substrate produces a uniform monolayer that can be used as a mask for depositing metals like gold to produce patterned surfaces to generate a localized surface plasmon for biosensing applications[18]. Other applications include nanostructured-nanopatterned titanium dioxide substrates to investigate biocompatible nature of metal oxide[19], developing 2D arrays of nanowires-nanopillars[17],etc.

A sound focusing system (acoustic lens) is a disc of sapphire whose axis is aligned parallel to the crystallographic c-axis. At the center of the one face of disc is a spherical cavity. This cavity provides the focusing actions and on the other face thin film of gold forming an electrode is deposited. A transducer i.e. an epitaxially grown Zinc Oxide (ZnO) is vacuum sputtering on this face of the sapphire disc. Active area of the transducer surface is defined by a small dot of gold (electrode), which is exactly opposite to the focusing surface. Plane acoustic waves generated by transducer travel through the disc and when they cross the spherical interface between the lens and the fluid are refracted towards the focus on the axis of the lens[20,21]. Focal length (*f*) of an AL immersed in water is similar to that in an optical system and can be calculated from equation 1-

$$f = \frac{r_o}{1 - n} \tag{1}$$

Where r_o is radius of curvature of the spherical surface and n is the ratio refractive index of the first and the second medium. This focusing effect of sound wave in aqueous environment can enable controlled convergence of microparticles towards the focal plane of the acoustic lens that helped in developing a uniformly assembled monolayer of polystyrene particles.

To drive the particles and have a stable monolayer of particles primarily depends on the acoustic radiation force generated by the AL towards the focal plane. This theory for acoustic radiation force was first proposed by Yosioka and Kawasima[22]. And its implementation to estimate acoustic pressure on micro-sized latex particles has been used by researchers working in the field of microfluidics[23]. More recently Henrik Bruus introduced few improvements to the original theory where acoustic radiation force is calculated by taking Scattering theory into consideration[24]. In an inviscid fluid the net acoustic radiation force F_{ac} on a small spherical particle is the gradient of an acoustic potential U_{ac} also known as Gor'kov potential[25],

$$F_{ac} = -\nabla U_{ac} \tag{2}$$

$$U_{ac} = \frac{4\pi}{3} R^3 \left[f_1 \frac{1}{2} \gamma_o \langle P_{in}^2 \rangle - f_2 \frac{3}{4} \rho_o \langle \vartheta_{in}^2 \rangle \right] \tag{3a}$$

where R is the radius of the particle having density ρ_p and compressibility γ_p is suspended in an inviscid fluid of density ρ_0 and compressibility γ_o. Potential U_{ac} to drive particles is also proportional to incoming density wave P_{in} and incoming velocity wave ϑ_{in}. The coefficients of scattering f_1 & f_2 are given by

$$f_1(\widetilde{\gamma}) = 1 - \widetilde{\gamma}, \quad with \quad \widetilde{\gamma} = \frac{\gamma_p}{\gamma_o}, \tag{3b}$$

$$f_2(\widetilde{\rho}) = \frac{2(\widetilde{\rho}-1)}{2\widetilde{\rho}+1}, \quad with \quad \widetilde{\rho} = \frac{\rho_p}{\rho_0} \tag{3c}$$

In our experiment acoustic frequency generated by AL is 89 MHz. This is the drive frequency that drives the particle forward in the direction parallel to acoustic wave. For velocity of sound in water at 1490 m/s, wavelength (λ) of acoustic wave driving the particles would be 16.74 microns. Particle used in this study are 2 micron in size and the above method for estimating acoustic radiation force are performed with an assumption $R << \lambda$. Velocity of the particle (v_p) can be calculated by drag force calculated from Stokes' law

$$F_{ac} = -6\pi\eta R v_p \tag{4}$$

There are two methods to drive particles towards the focal plane. In the first method, a continuous wave (CW) at a frequency of 89 MHz is generated by the AL and in another one, drive frequency of 89 MHz is mixed with 2Hz pulse. The pulsed (PL) frequencies give more control to drive particles up to few microns. Hence, the velocity of the particle per pulse with displacement of z is given by following expression,

$$v_p(z) = \frac{2\pi\phi R^2 E_{ac} \sin(2\pi)}{3z\eta} \tag{5a}$$

$$\phi(\widetilde{\rho}, \widetilde{\gamma}) = \frac{1}{3}\left[\frac{5\widetilde{\rho} - 2}{2\widetilde{\rho} + 1} - \widetilde{\gamma}\right] \tag{5b}$$

where η is the viscosity of fluid, ϕ is acoustophoretic contrast factor and E_{ac} is acoustic energy density. Theoretical calculations for estimating energy density are discussed in the following references[24,26,27].

In the following study an AL is developed as a Micro-Acoustic Trap (μAT). A continuous stream of acoustic wave generated from an AL is coupled with a low frequency pulse (2Hz). This mixing of frequencies resulted in high precision mobility of the beads towards the center of the acoustic focal plane (AFP). This controlled mobility also helped in formation of an assembled monolayer of microparticles suspended in the 3D in DI water. This methodology was also tested with live *Dictyostelium discoideum*(Amoebas). Here the mobility of the cells towards AFP is observed with a continuous acoustic wave at a drive frequency of 89 MHz. Here drive frequency is not coupled with 2 Hz pulses. With a highly focused acoustic beam one could also observe shriveling of a cell membrane, shrinking of a cell under a continuous wave of acoustic radiation and when a cell was pushed too hard against the glass substrate, its cell membrane got ruptured. In this study we have used an AL that is immersed in DI water that may have polystyrene beads or live cells. By mixing different frequencies, an AL one can be developed as a μAT that be used for microparticle assembly in 3D plus by using a focused continuous stream of acoustic waves one can segregate adherent and non adherent cells. A focused acoustic stream can be used investigate cell membrane and other nanomechanical properties.

Results

A Monolayer Assembly in 3D. Use of acoustical methods like OTs to control mobility of particles, cells and other micro-sized objects has become topic of interest during the last decade or so. Experimental work being conducted by various research groups is focused on achieving a maximum maneuverability of particles both in air and water. The objective of the current investigation is to study effect of focused acoustic beam on freely moving suspended micro-particles in aqueous environment (DI water). In most of the investigations an ATω are used to manipulate 2-3 beads at a time. This study demonstrates a methodology to systematically

manipulate large number of particles in aqueous environment. There are considerably complex hydrodynamic forces that play crucial role in mobility objects in water. Thus the worked discussed in this article got initiated with the objective to understand the flow of particles at the focal plane of the AL.

The experiment setup and schematic is shown in Figure 1(a) & 1(b) respectively. The lens is immersed in suspension of 2 micron sized polystyrene particles. The particle suspension also contains Triton-x, a nonionic surfactant to neutralize negative surface charge on the polystyrene beads. This prevents any non-specific adhesion between the particles and glass bottom of the fluid cell. The objective of the inverted microscope was underneath the glass bottom fluid cell and was used to focus on to the acoustic focal plane of the AL. The precise positioning of the AL is controlled via micomanipulator and was adjust to hover few micron above the glass bottom of the fluid cell. Continuous waveform that drives particles towards the focal plane of AL was generated by directly coupling function generator (FG) via amplifier to acoustic transducer. Distance of the focal plane from center of the spherical aperture of the AL was measured by fine adjustment in micromanipulator (with minimum divisions -10 microns). Therefore, the center of the acoustic focal plane was 1.06 mm ± 0.09 mm from the spherical aperture of the AL, which was visualized using inverted optical lens below the sample stage. As illustrated in the sketch in Figure 1(b) polystyrene beads freely float in DI water, were propelled towards the focal plane by vortex beam created by AL[28]. Motion of the particles is capture with high speed imaging system coupled to the optics of the inverted microscope. Polystyrene beads were driven at 1V drive amplitude at a frequency of 89 MHz and can be observed in supplementary movie-1. This is a 10 sec video with frame rate slowed down to 15fps. As illustrated in figure 1(b) microparticles are driven into AFP and are observed optically by inverted optical lens below the fluid cell. It is

important to note that optical focus should be aligned with AFP to observe motion of beads. Here one can observe that beads move into AFP from the top and move down towards the objective lens. Therefore, to best observe this effect, distance D between the aperture of AL and glass bottom of the fluid cell should be greater than the AFP (F). The fundamental mechanism that drives the particles in the direction of the acoustic wave is illustrated in figure 1(c). As discussed earlier, z is the displacement of particle in the direction of acoustic wave, R is radius of the polystyrene beads and λ is the wavelength of the incoming acoustic wave. ρ_p & γ_p are density and compressibility of the particle respectively. In an inviscid fluid, density and compressibility is defined by ρ_0 & γ_o respectively.

Due to the limitation of the optics, data required to estimate velocity and displacement of particles could only be determined in X & Y axis. Due to the mobility of particles vertically across the focal plane, parallel to Z-axis, it became an experimental limitation to measure the dynamics of the particle in the 3 dimensions simultaneously. Hence, for accurate estimation of velocity, displacement and other parameter associated with motion of particles, AL was driven at 2Hz pulsed frequency coupled with drive frequency of 89 MHz. The driving frequency was modulates at 3 different amplitudes of 0.5V, 1V and 1.5V. Pulsing the drive frequency, confines the mobility of beads in X & Y plane and power to drive particles is proportional to amplitude of the drive frequency. Minimal motion of the beads in Z-axis assisted recording displacement of styrene beads with each pulse. Here beads gently move across X & Y axis rather than moving across the Z-axis i.e. perpendicular to the direction of observation via objective lens. The hardware diagram for the assembly required to conduct such measurements is shown in Figure 2(a) and the corresponding timing diagram can be seen in Figure 2(b).

To capture instantaneous displacement of beads under pulsed acoustic waves, signal (exposure start time) is first drawn from the high-speed camera and then the signal is split into half (1/2) by frequency divider. A 5V split pulse is generated from the divider, which is synced with a 5V DC source and the camera. A 2Hz (20% duty cycle) pulse from low frequency FG is synced with divider signal and mixed with 89 MHz sin wave from high frequency FG via SMA mixer. The signal derived from the SMA is amplified to drive acoustic transducer (lens).

Hence, for accurate estimation of velocity, displacement and other parameter associated with motion of particles, AL was driven at 2Hz pulsed frequency with a drive frequency of 89 Mhz. Pulsing the drive frequency, limits mobility of beads in X & Y plane. Measurements were conducted by driving AL at three different voltages, 0.5V, 1V and 1.5V. Minimal motion of the beads in Z-axis facilitates recording displacement of styrene beads with each pulse.

Montage of data recorded with high-speed camera at 0.5V is shown in supplementary information SI Figure 1 and real time motion of particle under the influence of acoustic radiation pressure can be observed in supplementary movie-2. During the first 10 sec AL is off and Brownian motion among freely suspended particles can be observed. During next 30 sec acoustic pressure thrusts the particles towards the center of the frame i.e. center of acoustic focal plane. At 0.5 V power is just barely enough to overcome Brownian. Particles do move towards center of the frame but do not come in physical contact with each other. In the end when system is switched off beads revert back to their Brownian state.

For drive amplitude of 1V, transducer was driven for 40 sec. Acoustic pressure subdues the Brownian and particles are pushed towards the center with greater displacement. From both SI Figure 2 and supplementary movie- 3 one can observe that particles tend to arrange themselves as a loosely formed monolayer. From 35.76 sec onwards beads get arranged parallel to XY

plane. The wave fronts created by AL are circular in nature; this assembles beads as disc of particles in the center of the frame. On closer observation, beads are in random close pack (RCP) arrangement. Acoustic pressure is not high enough to pack beads in an orderly manner. During last 10 sec transducer is switched off and microparticles revert back to their brownian state and get dispersed.

Figure 3 is the montage for the 1.5V drive amplitude. Particle displacement towards the center of the frame is highest and with relatively insignificant brownian. In supplementary movie-4 one can observe an orderly formation of monolayer of polystyrene particles similar to NSL, only difference being that this monolayer of beads in suspended in aqueous environment where in NSL 2D array is formed on a solid substrate. It is at the end of ~30 sec acoustic excitation one can observe formation a suspended 2D monolayer. The complete assembly of the particles can be observed at 40.43 seconds (middle lower frame) in Figure 3. Thereafter, particles revert back to their Brownian state and the assembled monolayer gets dispersed.

The last frames for 30 sec (0.5V), 40 sec (1V) & 30 sec (1.5V) acoustic drive cycles can be observed in Figure 4(a), 4(b) & 4(c) respectively. Here one can observe that at assembly of particles only takes place at higher voltages, 1 V & above. Centrally assembled mass of beads at 1V in Figure 4(b) took 10 sec longer when compared with Figure 1(c) at 1.5V. At low voltages acoustic pressure is not high enough to construct an assembled monolayer. At drive amplitude of 1V assembled layer of beads is ~ 72 µm in diameter. The monolayer mass of particle formed at 1.5V is ~ 83 µm in diameter. Figure 4(d) is zoomed image of the central region in Figure 4(c), marked by dashed white arrow. Acoustic radiation pressure generated at 1.5V creates a hexagonal closed pack (HCP) lattice where density of particles is relatively high as compared to RCP arrangement with 1V drive amplitude.

To further confirm assembled layer 2 µm is not a multilayered structure, third dimensional imaging along the Z-axis was performed with confocal setup. A Z-stack of images was collected over a range of 38 µm. Each Z-slice is collected with resolution of 1 micron. There are 38 slices in one stack that can be observed in supplementary information SI Figure 3. A monolayer of 2 micron beads can be observed at slice -24 in Figure 5(a), with no other layered structures immediately above and below the disc of microparticles. Though on closer inspection of stack of 38 images relieved an incomplete layer of beads can be observed in slice-33, shown in Figure 5(a). The same is explained in sketch in Figure 5(b) and this second layer of beads is 8 ±1 µm below the fully assembled 2D array of particles. As discussed earlier wavelength of waves generated by our AL is 16.74 µm. Therefore, second layer so formed is at half of the wavelength of the acoustic wave generated by the transducer at a frequency of 89 MHz. Acoustic waves are basically compression waves, therefore tight packing of the beads as shown in figure 4(c) takes place at the local region of compression and the second loosely formed layer shown in slice 33 in figure 5(a) gets formed at the local region of rarefaction. Distance between centers of the compressed (stacked maxima) and rarefaction (stacked minima) is half of the wavelength. This correlated with our observation of formation a second partially assembly layer of beads at a distance of 8 micron. This effect is similar to previously reported standing wave acoustic levitation of particles in air by Hertz in the year 1995[29]. Since then, number of groups have experimented with this concepts have even tried to levitate water droplets by developing acoustic potential wells with help more one acoustic transducers[9,30].

This partial assembly of particles could have grown to a fully assembled array if the system was driven longer than 30 sec. It's important to highlight fact that 3D reconstruction of Z-stack is not possible, only slice by slice imaging is possible. The central disc of assembled particles is stable

as long as it is under certain degree of acoustic pressure. Therefore, each image in a Z-stack is slightly different from the previous one, as disc of microparticles is not stationary and newer particles continuously merge with the central structure. For successful 3D reconstruction from Z-stack, the sample under observation should be motionless which is not possible with the <mark>current experimental setup.</mark>

It's difficult to estimate time required to assemble a monolayer. There are number of factor that affect duration of particle assembly at the acoustic focal plane. It not only depends on the acoustic power but also on density of beads in aqueous media. Size, shape and density of particles can have considerable impact on particle assembly. Due to periodic bombardment of acoustic waves, beads moves in stepwise manner, in form of regular jumps. Microparticle tracks with their respective XY coordinates in their 2D frame are shown in Figure 6(a). Tracks of each beads has a different color. Red arrows indicate the direction of motion of particles towards center of the frame, which is also center to the AFP. Tracks start towards the outer edges of the frame i.e. the point at which beads enter optical field of view. The tracks stop at the center of the frame where beads get assembled as a disc shaped 2D lattice of latex particles. Blue colored beads are overlaid over the particle tracks for the purpose of illustration. Beads assemble in the center of the frame and periodic thrust from each pulse can be seen in form kinks in each of the tracks.

Randomly selected displacement data of 4 beads from 1.5 V drive amplitude tracks is shown in Figure 6(b). Particle displacement with respect to each frame (in X-axis) corresponds to displacement in micrometer (μm) (in Y-axis). It was interesting to observe that the maximum displacement of particles happens during the first acoustic pulse and with the subsequent acoustic pulses displacement of particles gradually decreases. The only possible explanation to

this observation is increase in the proximity of particles with each acoustic pulse. Initially polystyrene beads are homogenously suspended in DI water. But with each pulse, proximity of beads increases as they move towards the center of AFP (in the center of the frame) and get incorporated into microparticle assembly. This also increases hydrodynamic drag, which in turn reduces the net displacement of the particles when they are forming a suspended monolayer in the center of the frame. This effect can also be observed in Supplementary Movie-4.

Histogram of velocities of all the beads is shown in Figure 6(c). All Velocities at 1.5V drive amplitude (red marker) have maximum velocity > 200 µm/s. For 1V (green marker) and 0.5V (blue marker) observed maximum velocity goes up to 150 µm/s. For lower velocities there is a consistent peak at all drive amplitudes suggesting brownian motion during the resting phase between the two acoustic pulses. Any deviation from the path travelled by beads from outer edges of the frame towards the center of the frame was measured as All Delta Normal (ADN) angles. Angularity in the path travelled by each bead can be observed from Figure 6(d). For all magnitudes All Delta Normal (ADN) angle, count peaks at zero degree. This implies that there is minimal deviation from the path travelled by the beads until they merge with microparticle disc in the center of the frame. Small difference in counts at different drive amplitudes is merely due to different number of beads present in the frame before switching on AL.

Live Cell Segregation and Manipulation. To further explore applications of above discussed µAT setup, live *Dictyostelium discoideum* (amoebas) were used for manipulation as compared with polystyrene beads. Amoebas were fluorescently labelled with GFP-Lifeact[31] vector. Unlike styrene beads, cells are not freely floating in HL5 media plus their average size is between 8-10 microns. Here the objective was segregation of non-adherent or loosely bound cells from the cell adhered on the glass surface. Therefore, by taking into account these factors, AL was driven at a

continuous frequency of 89 MHz. Frequencies generated with AL were not coupled with pulsed frequency (of 2Hz) as discussed earlier. As the dimension of the cells were lot bigger and higher drive amplitude of 2 V was used for manipulating live cell.

The key factor in the above-described measurement is the knowledge of the placement of AFP within the optical frame and its recording by the objective below the fluid cell. Displacement tracks of amoebas are overlaid onto fluorescent image is shown in Figure 7. As only few cells were loosely adhered on to the glass surface, the acoustic focal point was placed near the lower left hand side of the frame in order to observe maximum mobility of the cells. As shown in the Figure 7 only cells that were not stuck on the glass surface showed some degree of mobility. Two cells on the lower half of the image moved towards the AFP and third on the center upper half of the image took the path with least obstruction from the adjacent cells. Isolated tracks of three cells with the dimensions in microns are shown in SI Figure 4.

Further studies revealed that the under the influence of strong acoustic pressure, cells with relatively weaker actin cytoskeleton, a shriveling effect on the cell membrane can be observed. Similarly cells with even weaker cytoskeleton can get compressed (shrink) with continuous onslaught of sound waves. Dimension of one such amoeba got reduced by 40 % is shown in Figure 8 and in Supplementary Movie-6. In the observation frame, one amoeba rotates by ~20° is highlighted by angled yellow lines. In another observation loosely bound amoebas get pushed against the glass surface and acoustic pressure was strong enough to rupture its cell membrane (Figure 9 & Supplementary Movie-7). It is important to note that the observations discussed in Figure 8 & 9 highlight the effects continuous sound waves generated by AL. And out of large number of cells observed only amoebas having weaker cytoskeletal network are not able to resist any mechanical force exerted by sound waves.

Discussion

In this study we have presented a novel 3D μAT for manipulating particles in aqueous environment. As discussed earlier most groups have developed highly sophisticated assembly of transducers for manipulating particles. But our methodology is lot simpler and requires only one acoustic lens to mobilize and assemble microparticles in the region of interest. This technique can also be extended to non-aqueous environment. Particle dynamics in transparent organic liquids can have significant impact in material sciences. At higher magnitudes and with slightly larger AL aperture one can develop a high throughput system to automate particle assembly for microfluidic systems. The novel technique present in this article would help design more sophisticated μAT with applications in both material and biological sciences.

A monolayer of beads formed at the end of 1.5V drive amplitude cycle, if polymerized can also be used as mesh for filtering particles. Another interesting application would be to segregate particles having different shapes and sizes. A particle sorting system, which can segregate particles on the basis of their dimensions, can be used in water filtration systems to remove coarse impurities. Further studies are required if we want to manipulate objects having molecular dimensions like multimeric proteins, DNA origami or any other large molecular

In this study we have demonstrated that it is possible to distort cells and also move them towards a region of interest. With further improvement in the current state of the technology, one can investigate nanomechanical properties of large number of cells in one go. In more recent developments, not just acoustic lenses but also a surface acoustic wave (SAW) device are being used as ATω[32]. A SAW device can be used for aggregating large number of cells to grow multicellular spheroidal cultures. Exactly opposite to our measurements discussed in figure 8 &

9, Guo *et al* attempted to modulate adhesion of cell on to Surface Acoustic Wave (SAW) device[33]. During the acoustic drive cells kept hovering over its surface. Once the device was switched off, cells start adhering to the surface of the devices. With the methods discussed in this article, one can quantify mechanical properties of soft biological materials. The work presented in this article can have significant impact in the field of fluid dynamics, cell nanomechanics, and similar acoustic levitation systems currently being experiment by various research groups. More systematic details associated with particle dynamics will be discussed in future articles.

Methods

Microparticle Suspension

2 µm polystyrene spheres where purchased from Thermo Fisher Scientific. 5µl of sphere concentrate was diluted in 1 ml of milli-q water. To the suspension 2 µl of Triton-x surfactant was added and particle suspension was placed in glass bottom fluid cell. Aperture of the AL was immersed in the suspension and the AL was held at it place on a custom build micro-meter stage. Optomechanical components controlling minute motion of AL in 3D where purchased from Thor-Labs. Imaging was performed with inverted microscope in bright field with 40x objective.

Acoustic Lens Measurements

The Acoustic lens (100 MHz; 60° aperture angle, KSI Germany) was driven at 89 MHz with CW (Hewlett Packard 8647a signal generator) and PL (Agilent 33250A, waveform generator) frequencies. Signals from the two generators were mixed using SMA mixer (Watkins Johnson WJ M1A 3-1000 MHz). Signals from the waveform generators and SMA mixer were amplified using ENI 350L RF Power Amplifier (Bell Electronics, Renton WA). During CW measurements, lens was operated at 1V. For PL frequencies lens was operated at 0.5V, 1V and 1.5V. For 0.5V and 1.5V measurements, movie data sets were collected at 10sec off/ 30sec on/ 10sec off. For 1V measurements AL was driven 10 sec longer and movie data set was collected with AL at 10sec off/ 40sec on/ 10sec off.

Dictyostelium Transformation and Cell Culture

Dictyostelium discoideum Ax2 cells were transformed with Lifeact [31] by electroporation as described previously[34]. Briefly, a near confluent 60 mm plate of cells was harvested and washed twice with ice-cold H-50 buffer (20 mM HEPES, 50 mM KCL, 10 mM NaCl, 1 mM $MgSO_4$, 5 mM $NaHCO_3$, 1 mM NaH_2PO_4 pH 7.0) and re-suspended in enough H-50 to bring the cells to a titer of approximately 1 x 10^7 cells/ml. About 5 µg of plasmid DNA was mixed with 100 µl of cells, transferred to an ice cold 0.1-cm electroporation cuvette and pulsed twice at 600 V and 50 µF using an ECM 630 Electro Cell Manipulator (BTX, San Diego, CA). After a 5 min incubation on ice the cells were transferred to 60 mm Petri dishes containing 5 ml of HL5 medium (10 g BBL™ Thiotone™ E peptone, (Becton Dickinson, and Company, Sparks, MD) 10 g Glucose, 5 g Yeast Extract, 0.35 g Na_2HPO_4, 0.35 g KH_2PO_4, 0.1 mg/ml ampicillin, 0.1 mg/ml dihydrostreptomycin, pH 6.5)[35] and incubated at 22°C for 24 hrs before drug selection. Fluorescent colonies were picked manually after 7–10 days. Cells were pipetted onto a glass

substrate and were allowed to settle for 5-10 mins and were used for further studies with μAT. All clones were maintained in HL5 medium.

Conflict of Interest

The authors state no conflict of interest.

Acknowledgements

References

1. Ashkin, A. Acceleration and Trapping of Particles by Radiation Pressure. *Phys. Rev. Lett.* **24,** 156–159 (1970).

2. Ashkin, A., Dziedzic, J. M., Bjorkholm, J. E. & Chu, S. Observation of a single-beam gradient force optical trap for dielectric particles. *Opt. Lett.* **11,** 288–290 (1986).

3. Ashkin, A., Dziedzic, J. M. & Yamane, T. Optical trapping and manipulation of single cells using infrared laser beams. *Nature* **330,** 769–771 (1987).

4. Wu, J. Acoustical tweezers. *J. Acoust. Soc. Am.* **89,** 2140–2143 (1991).

5.   Foresti, D. & Poulikakos, D. Acoustophoretic Contactless Elevation, Orbital Transport and Spinning of Matter in Air. *Phys. Rev. Lett.* **112,** 24301 (2014).

6.   Bruus, H. *et al.* Forthcoming Lab on a Chip tutorial series on acoustofluidics: Acoustofluidics—exploiting ultrasonic standing wave forces and acoustic streaming in microfluidic systems for cell and particle manipulation. *Lab Chip* **11,** 3579–3580 (2011).

7.   Chou, C.-H. & Khuri-Yakub, B. T. in *Review of Progress in Quantitative Nondestructive Evaluation* (eds. Thompson, D. O. & Chimenti, D. E.) 677–685 (Springer US, 1987). doi:10.1007/978-1-4613-1893-4_76

8.   Gesellchen, F., Bernassau, A. L., Dejardin, T., Cumming, D. R. S. & Riehle, M. O. Cell patterning with a heptagon acoustic tweezer - application in neurite guidance. *Lab Chip* **14,** 2266–2275 (2014).

9.   Marzo, A. *et al.* Holographic acoustic elements for manipulation of levitated objects. *Nat. Commun.* **6,** 8661 (2015).

10.   Melde, K., Mark, A. G., Qiu, T. & Fischer, P. Holograms for acoustics. *Nature* **537,** 518 (2016).

11.   Baresch, D., Thomas, J.-L. & Marchiano, R. Observation of a Single-Beam Gradient Force Acoustical Trap for Elastic Particles: Acoustical Tweezers. *Phys. Rev. Lett.* **116,** 24301 (2016).

12.   Courtney, C. R. P. *et al.* Independent trapping and manipulation of microparticles using dexterous acoustic tweezers. *Appl. Phys. Lett.* **104,** 154103 (2014).

13.   Spadoni, A. & Daraio, C. Generation and control of sound bullets with a nonlinear

acoustic lens. *Proc. Natl. Acad. Sci.* **107,** 7230–7234 (2010).

14. Veronick, J. A. *et al.* Mechanically Loading Cell/Hydrogel Constructs with Low-Intensity Pulsed Ultrasound for Bone Repair. *Tissue Eng. Part A* **24,** 254–263 (2017).

15. Veronick, J. *et al.* The effect of acoustic radiation force on osteoblasts in cell/hydrogel constructs for bone repair. *Exp. Biol. Med.* **241,** 1149–1156 (2016).

16. Hulteen, J. C. & Van Duyne, R. P. Nanosphere lithography: A materials general fabrication process for periodic particle array surfaces. *J. Vac. Sci. Technol. A* **13,** 1553–1558 (1995).

17. Colson, P., Henrist, C. & Cloots, R. Nanosphere lithography: a powerful method for the controlled manufacturing of nanomaterials. *J. Nanomater.* **2013,** 21 (2013).

18. Jensen, T. R., Malinsky, M. D., Haynes, C. L. & Van Duyne, R. P. Nanosphere Lithography: Tunable Localized Surface Plasmon Resonance Spectra of Silver Nanoparticles. *J. Phys. Chem. B* **104,** 10549–10556 (2000).

19. Vyas, V., Podestà, A. & Milani, P. Probing Nanoscale Interactions on Biocompatible Cluster-Assembled Titanium Oxide Surfaces by Atomic Force Microscopy. *J. Nanosci. Nanotechnol.* **11,** 4739–4748 (2011).

20. Briggs, A. & Kolosov, O. *Acoustic microscopy*. **67,** (Oxford University Press, 2010).

21. Zhao, X. *et al.* Quantifying Micro-mechanical Properties of Soft Biological Tissues with Scanning Acoustic Microscopy. *Mater. Res. Soc. Symp. Proc.* **1301,** mrsf10-1301-oo13-08 (2011).

22. Yosioka, K. & Kawasima, Y. Acoustic radiation pressure on a compressible sphere. *Acta*

Acust. united with Acust. **5,** 167–173 (1955).

23.   Yasuda, K. & Kamakura, T. Acoustic radiation force on micrometer-size particles. *Appl.*

       Phys. Lett. **71,** 1771–1773 (1997).

24.   Bruus, H. Acoustofluidics 7: The acoustic radiation force on small particles. *Lab Chip* **12,**

       1014–1021 (2012).

25.   Gor'Kov, L. P. On the forces acting on a small particle in an acoustical field in an ideal

       fluid. in *Sov. Phys. Dokl.* **6,** 773–775 (1962).

26.   Dual, J. & Moller, D. Acoustofluidics 4: Piezoelectricity and application in the excitation

       of acoustic fields for ultrasonic particle manipulation. *Lab Chip* **12,** 506–514 (2012).

27.   Dual, J. & Schwarz, T. Acoustofluidics 3: Continuum mechanics for ultrasonic particle

       manipulation. *Lab Chip* **12,** 244–252 (2012).

28.   Hill, M. A one-sided view of acoustic traps. *Physics (College. Park. Md).* **9,** 1–2 (2016).

29.   Hertz, H. M. Standing-wave acoustic trap for nonintrusive positioning of microparticles.

       J. Appl. Phys. **78,** 4845–4849 (1995).

30.   Hong, Z. Y. *et al.* Dynamics of levitated objects in acoustic vortex fields. *Sci. Rep.* **7,** 7093

       (2017).

31.   Riedl, J. *et al.* Lifeact: a versatile marker to visualize F-actin. *Nat. Methods* **5,** 605 (2008).

32.   Chen, K. *et al.* Rapid formation of size-controllable multicellular spheroids via 3D

       acoustic tweezers. *Lab Chip* **16,** 2636–2643 (2016).

33.   Guo, F. *et al.* Controlling cell–cell interactions using surface acoustic waves. *Proc. Natl.*

Acad. Sci. U. S. A. **112,** 43–48 (2015).

34. Pang, K. M., Lynes, M. A. & Knecht, D. A. Variables Controlling the Expression Level of Exogenous Genes in Dictyostelium. *Plasmid* **41,** 187–197 (1999).

35. Watts, D. J. & Ashworth, J. M. Growth of myxamoebae of the cellular slime mould Dictyostelium discoideum in axenic culture. *Biochem. J.* **119,** 171–174 (1970).

Micro-Acoustic-Trap (µAT) for Microparticle Assembly in 3D

Varun Vyas[1(✉)], Michael Lemieux[3], David A. Knecht[3], Oleg Kolosov[2], Bryan D. Huey[1(✉)]

[1]Materials Science and Engineering Department, University of Connecticut, Storrs, CT 06269, United States

[2] Department of Physics, Lancaster University, Lancaster LA1 4YB, UK

[3]Deprtment of Molecular and Cell Biology, University of Connecticut, Storrs, CT 06269, United States
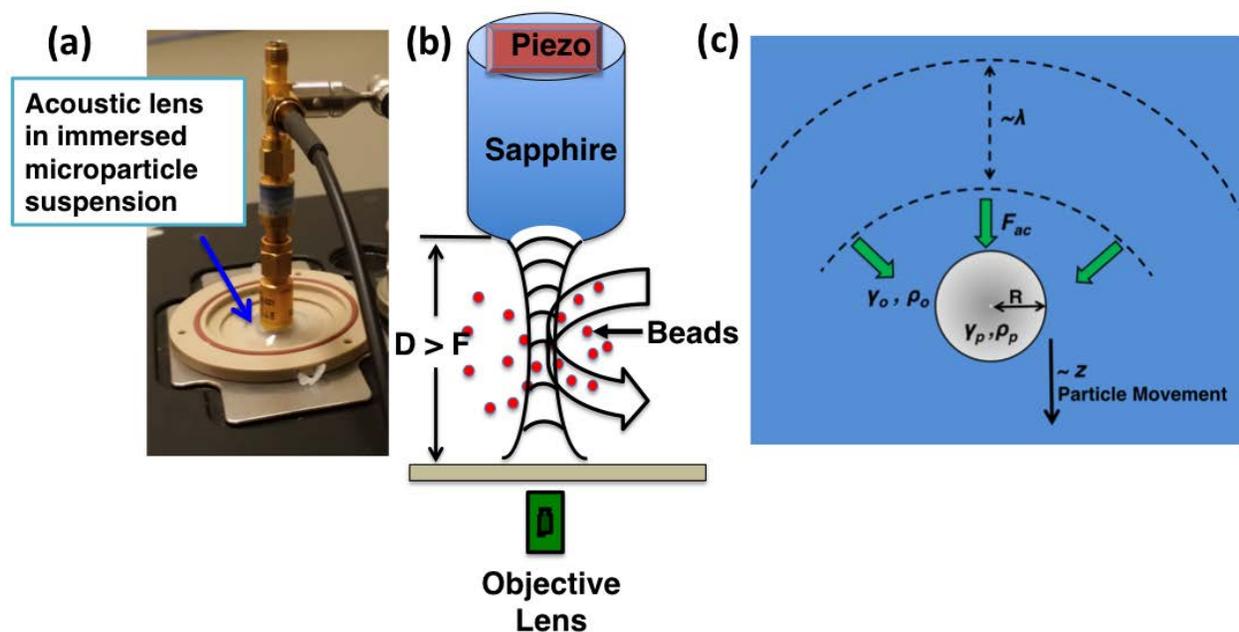
Figure 1. Acoustically driven self assembly of microstructures in liquid. **(a)** Oblique picture of experimental assembly, with acoustic lens submerged in DI water containing a suspension of 2 micron diameter polystyrene particles. **(b)** Experimental schematic, identifying the underlying coverslip and objective lens for inverted optical microscope and z-stack imaging to track particle positions and mobility before, during, and after acoustic excitation. D- distance between the acoustic lens and the glass substrate, controllable with a separate micromanipulator (not shown); F- Distance to acoustic focal plane, fixed at ~1.06 mm from the aperture and therefore positionable at or above the substrate; red dots demonstrate PS beads. **(c)** Illustration outlining the fundamental mechanism of planar microparticle assembly via acoustic pressure from above.
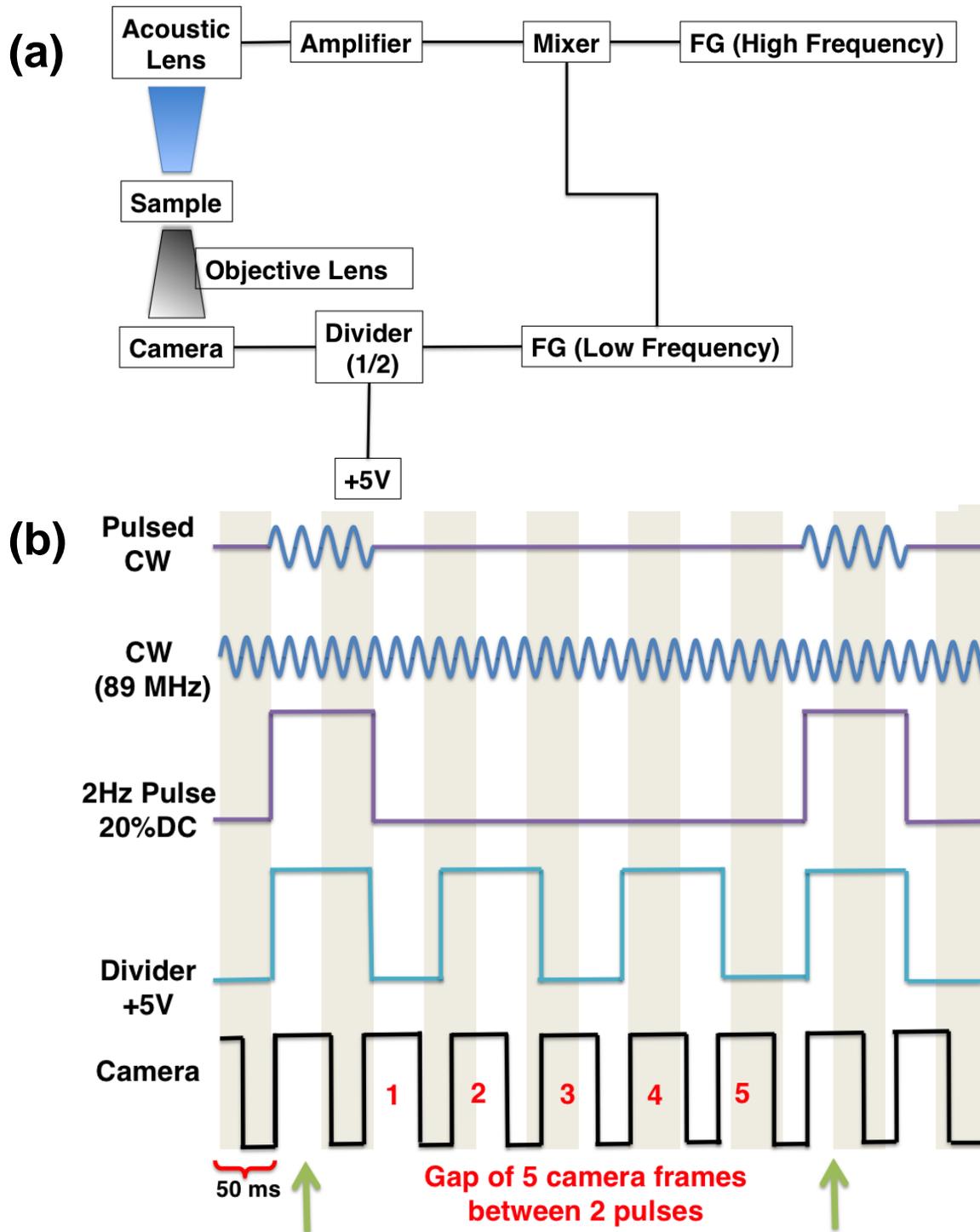
Figure 2. Hardware layout and diagram of acoustic and imaging timing for directly monitoring acoustic self assembly *in situ*. **(a)** Configuration for acoustic lens to generate acoustic pressure via a pulsed carrier wave, with a synchronized camera for visualization. **(b)** Timing diagram for the acoustic pulse, acoustic carrier wave, and camera acquisition signals.
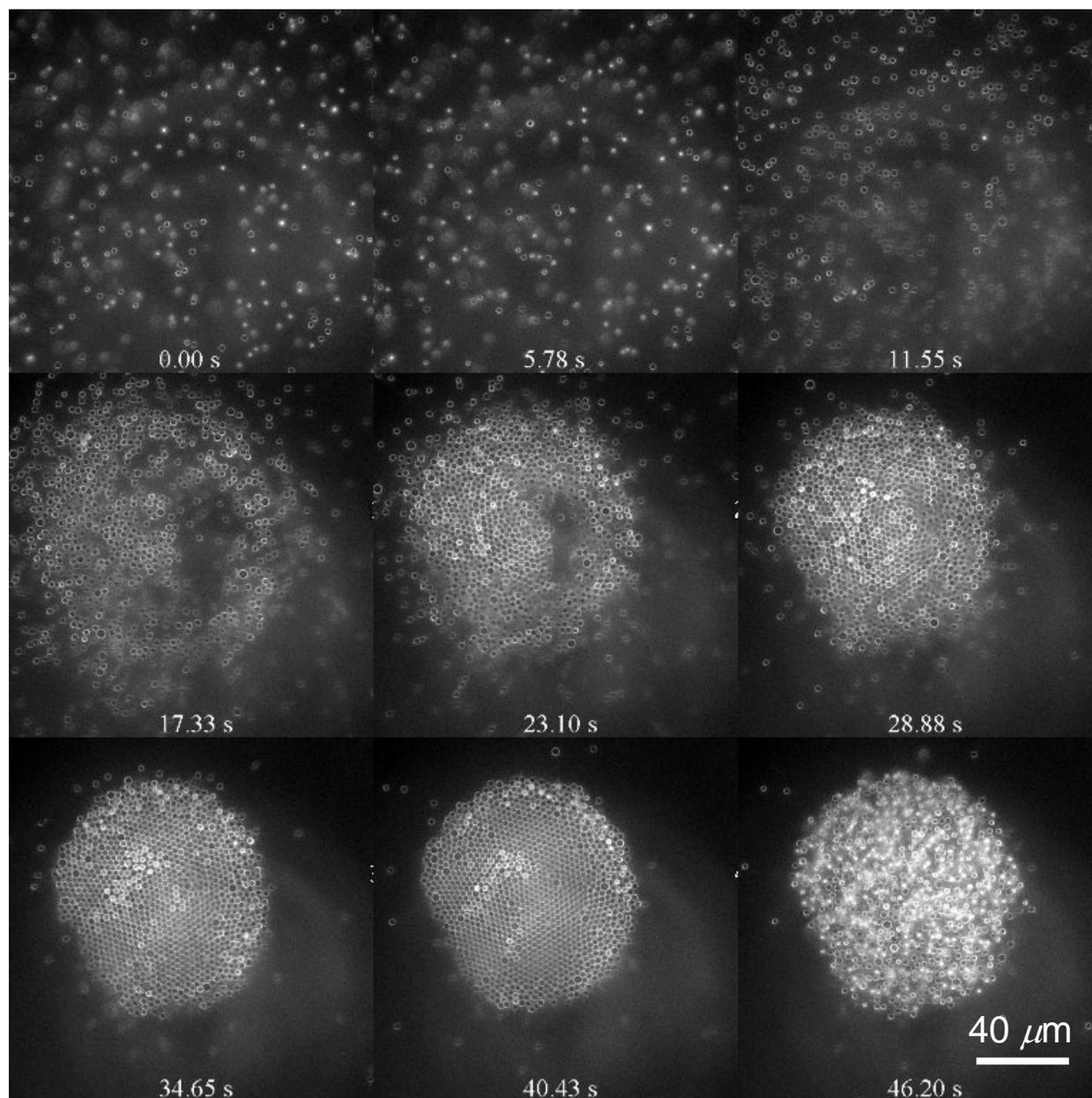
Figure 3. Optical image montage for polystyrene microparticles during acoustic excitation with 1.5V drive amplitude, clearly revealing self assembly at the acoustic focal point within ~30 seconds. The acoustic excitation is completed at 40.43 seconds (middle lower frame), beyond which disassembly appears to occur in all 3 dimensions via Brownian motion. Equivalent montages for lower drive cycles are provided in the SI.
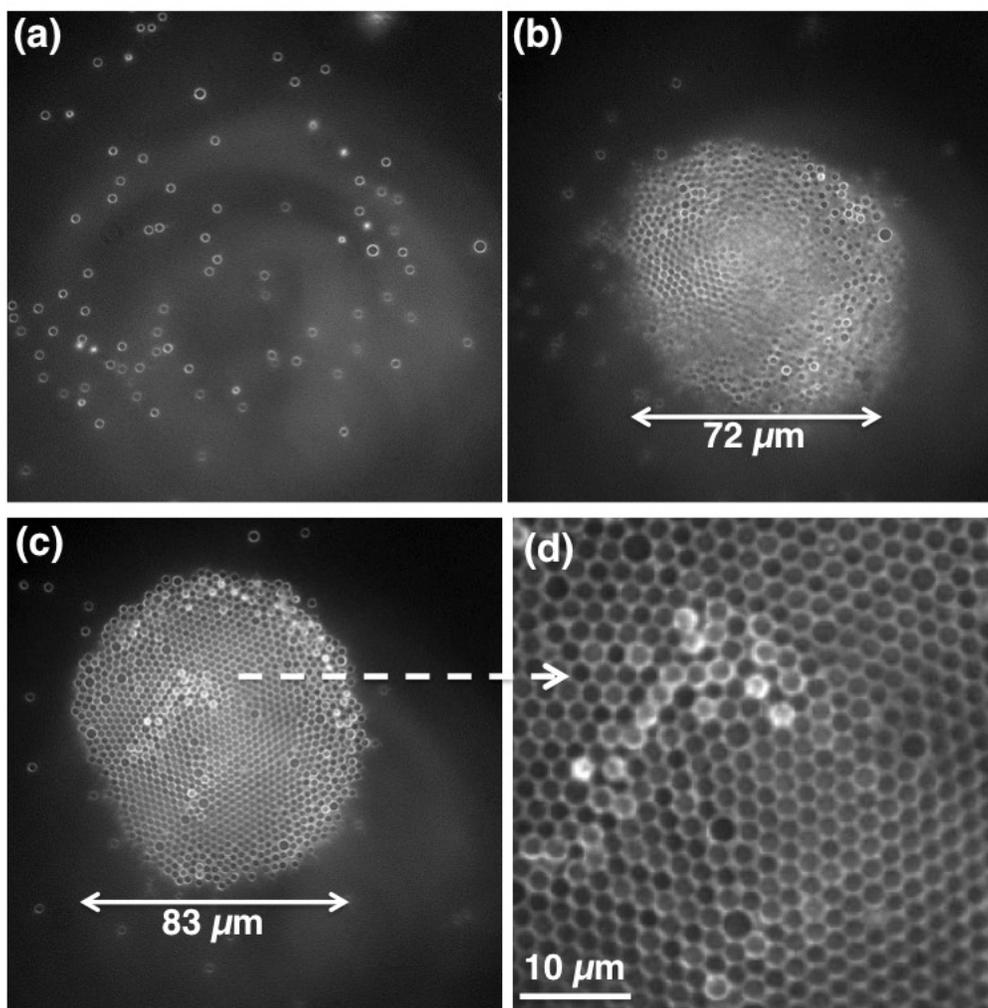
Figure 4. Summary of self-assemblies at acoustic focal point immediately following as much as 60 seconds of acoustic excitation, for drive magnitudes of (a) 0.5 V (b) 1 V and (c) 1.5 V. Higher optical magnifications as indicated (d) reveal clear 2-dimensional close packing of the 2 micron particles, with 'microstructural' defects initiated by PS spheres with atypical diameters.
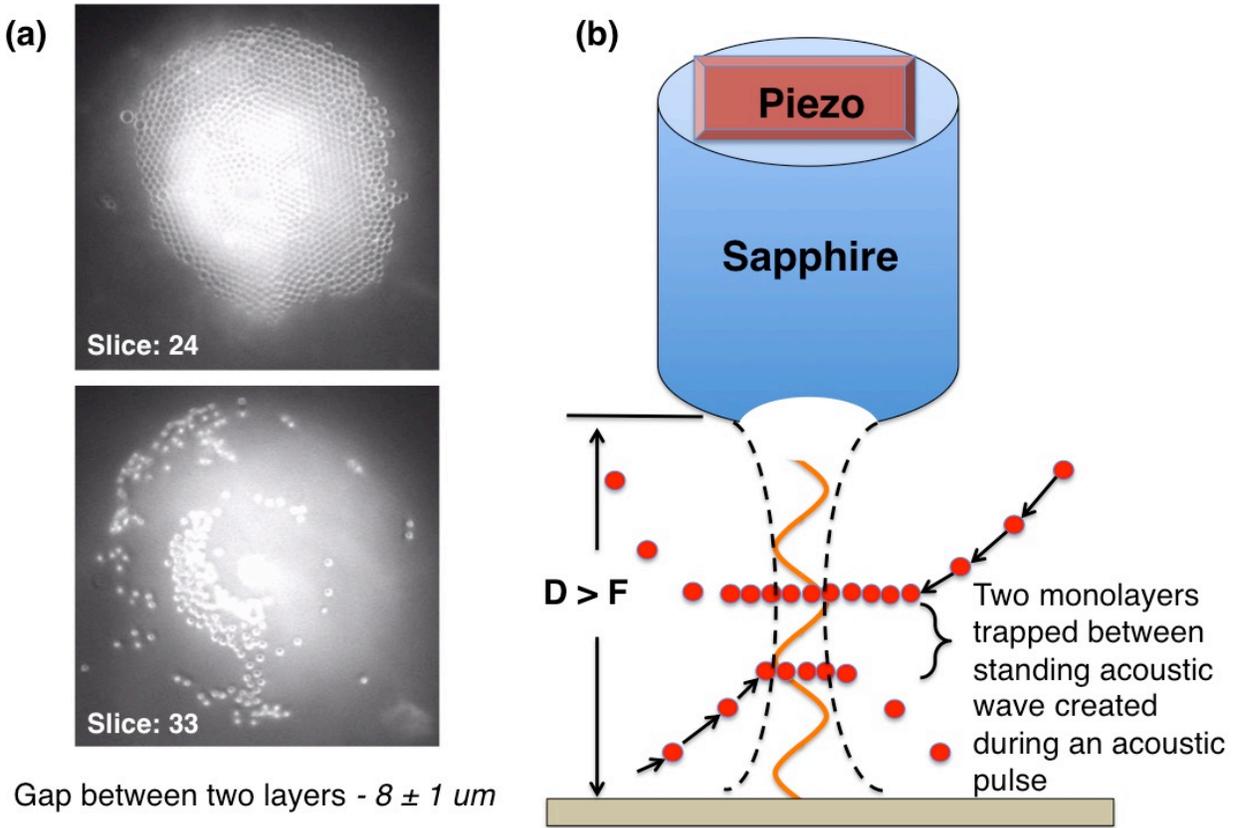
Figure 5.(a) Epifluorescence images at distinct focal planes demonstrating partial assembly of a second self assembled layer of microparticles (Slice:33) that is 8 ±1 µm below the primary self assembled microparticle disc (Slice: 24). The images are acquired within 90 milli-seconds of each other. **(b)** Schematic illustrating formation of the two different layers, driven with a 1.5 V amplitude as in Figure 3. The discrete non-contacting separation between the two layers is equal to the standing wavelength for the carrier wave frequency of 89 MHz and therefore results from stacked minima in the acoustic pressure (adjacent nodes in the Gor'kov potential).
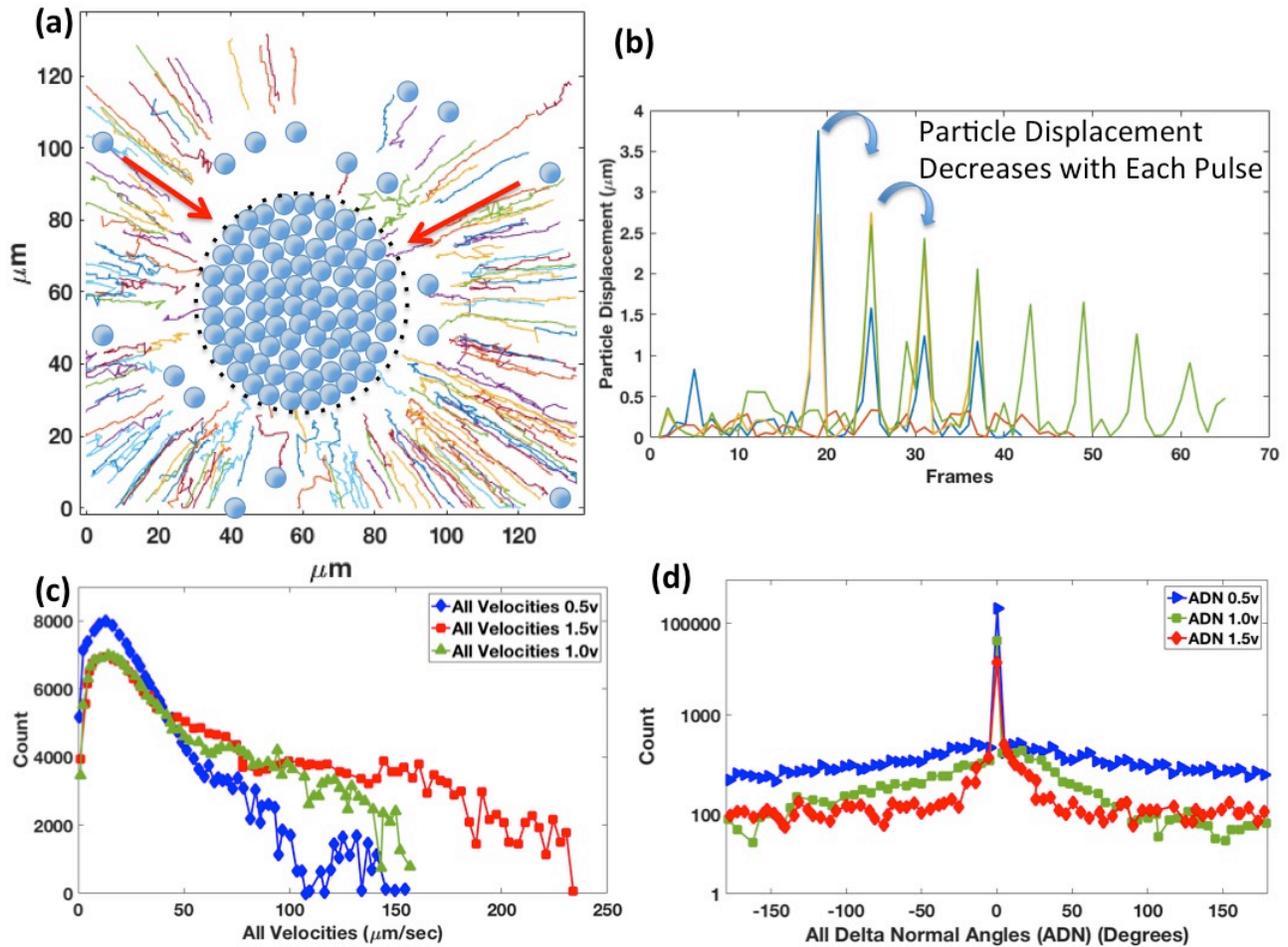
Figure 6. Analysis of particle self-assembly in acoustic pressure field, based on montage of ??? images during acoustic excitation as in Figure 3. **(a)** XY positions of particle tracks caused by 1.5 V amplitude of pulsed acoustic excitation. Blue beads are schematically added (not to scale) to demonstrate particle assembly in the center of the field of view in response to radial acoustic forces as indicated by overlain arrows. Subtle discontinuities in the particle tracks result from the 2 Hz pulse frequency, which imparts entropy via Brownian motion. The resulting periodic random walks are hypothesized to optimize the formation of close-packed monolayers by enabling particles to fill vacancies and heal other microstructural defects. **(b)** Representative displacement data of four distinct beads from (a). The effects of the pulsed radiation pressure are especially apparent for two of the particles considered. Before these particles are captured by the acoustic pressure field their displacements are small, and once captured the

displacements diminish as the particle becomes incorporated into the assembly. **(c)** Histogram of velocities for all tracked particles in all image frames during acoustic excitation. The velocity for the fastest recorded particles increases ~2.5x with a 3x increase in the driving amplitude as indicated. The peaks at ~10 um/sec result from Brownian motion, which is detected in all 3 cases based on images captured between the acoustic pulses. **(d)** The directionality of the acoustic driving force is quantified by a histogram of the changes (delta) in particle directions between every consecutive image frame. Higher driving amplitudes (acoustic pressures) clearly drive particles more effectively towards the focal point. Between pulses, randomly vectored Brownian motion dominates instead of any oppositely oriented recovery, as revealed by the angle-independent baseline for all three datasets.
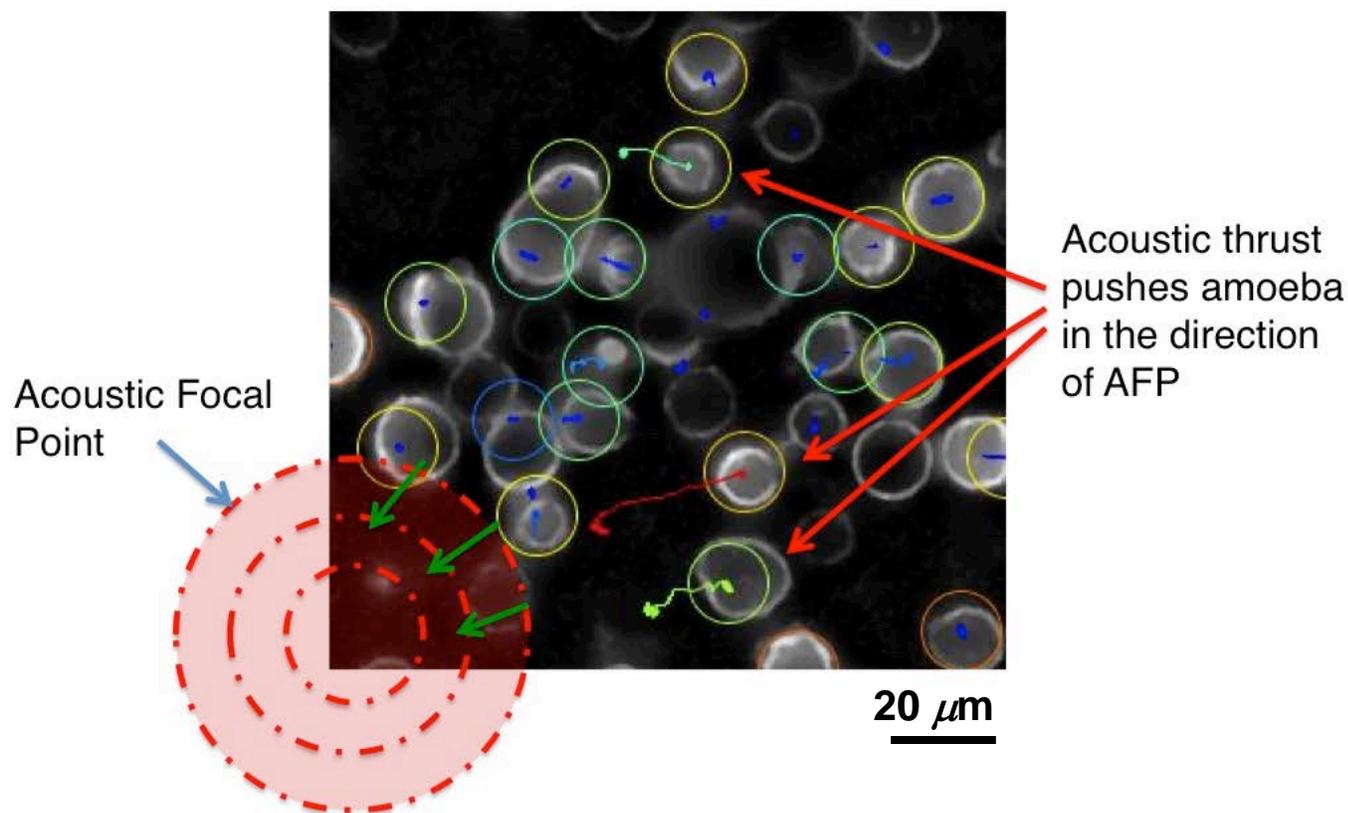
Figure 7. Displacement tracks of ~25 distinct *Dictyostelium discoideum* upon acoustically driving the Amoebas towards the acoustic focal point, including a sketches of the AFP location and acoustic pressure vectors. This is overlaid on a fluorescence image acquired just before assembly—the Amoeba membranes are GFP active and therefore outline the bacterial outer walls. Most amoebas are adhered to the glass surface and do not move appreciably. Two move substantially towards the Acoustic Focal Point in response to the acoustic thrust (identified by solid arrows). One appears to do so more circuitously due to a cluster of Amoebas hindering its direct path to the AFP (identified by a dashed arrow).
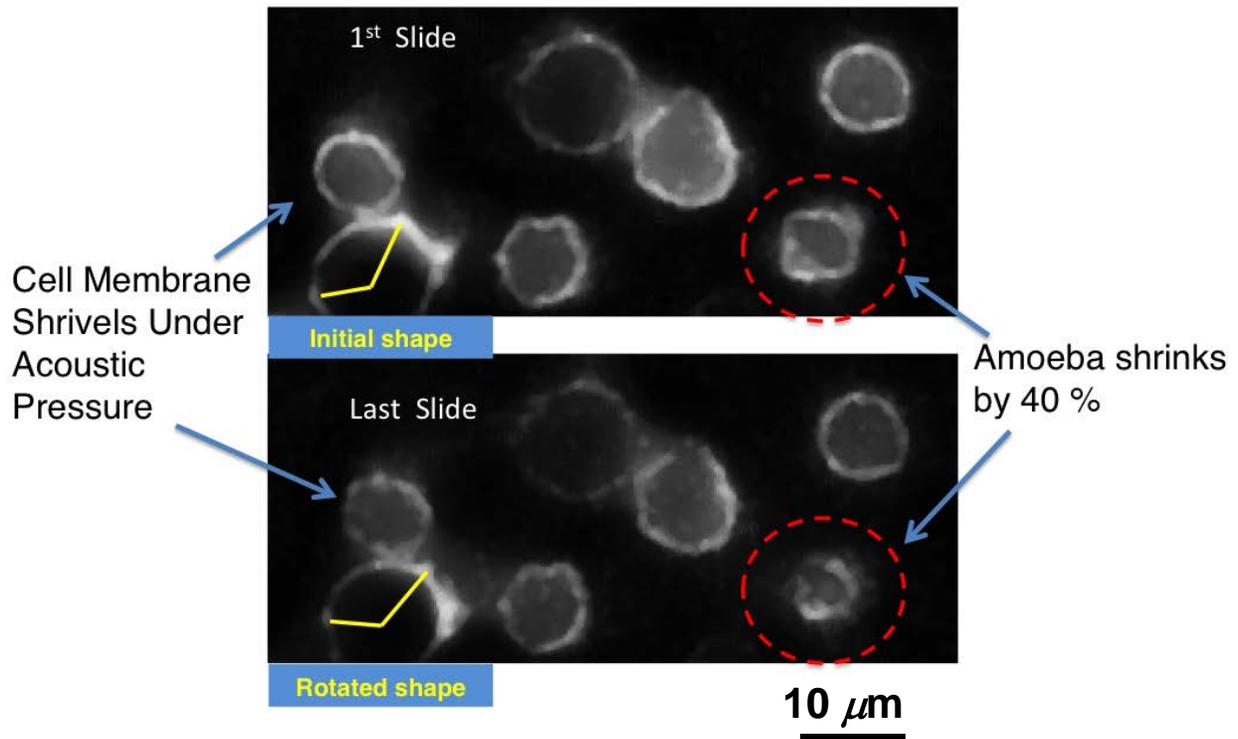
Figure 8. Distortion of amoeba membranes upon continuous acoustic pressure, including one amoeba (highlighted by the dashed oval) that experiences an ~40% decrease in diameter and another that rotates ~ 20° (highlighted by angled yellow lines).
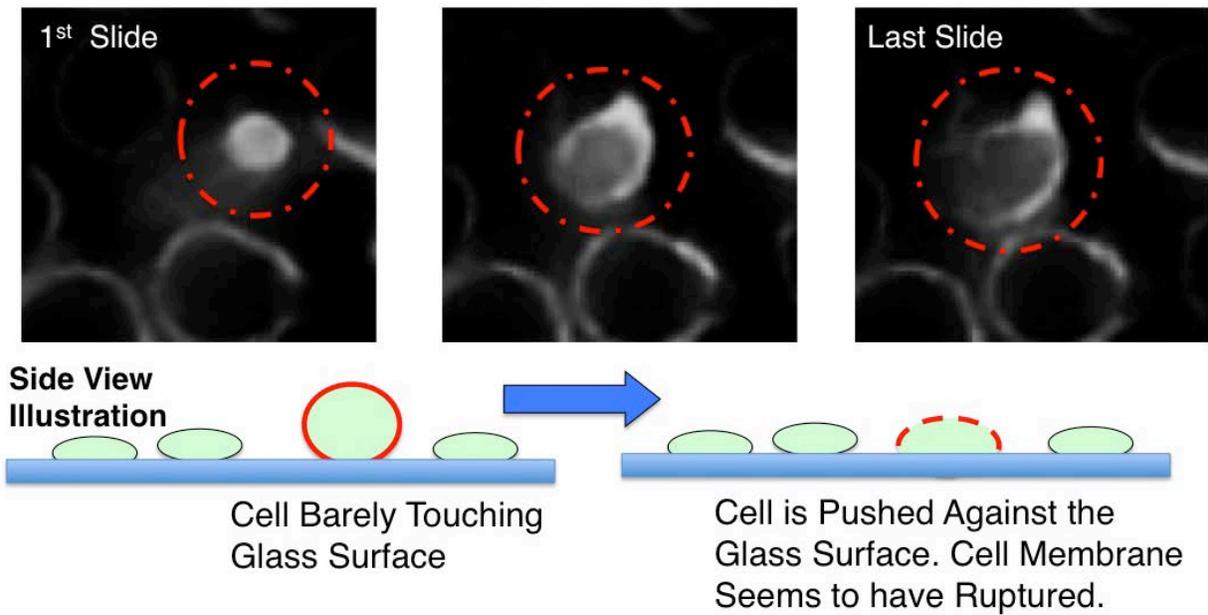
Figure 9. An Amoeba initially loosely adhering to the glass coverslip (highlighted by dotted overlay) is pressed onto the substrate during acoustic actuation, increasing the contact area as displayed schematically. This can encourage adhesion [there's a ref for this in one of the PNAS articles by Huang et al], or lead to cell rupture.

Supplementary Information

Micro-Acoustic-Trap (μAT) for Microparticle Assembly in 3D

Varun Vyas[1(✉)],Michael Lemieux[3], David A. Knecht[3], Oleg Kolosov[2], Bryan D. Huey[1(✉)]

[1]Materials Science and Engineering Department, University of Connecticut, Storrs, CT 06269, United States

[2] Department of Physics, Lancaster University, Lancaster LA1 4YB, UK

[3]Department of Molecular and Cell Biology, University of Connecticut, Storrs, CT 06269, United States
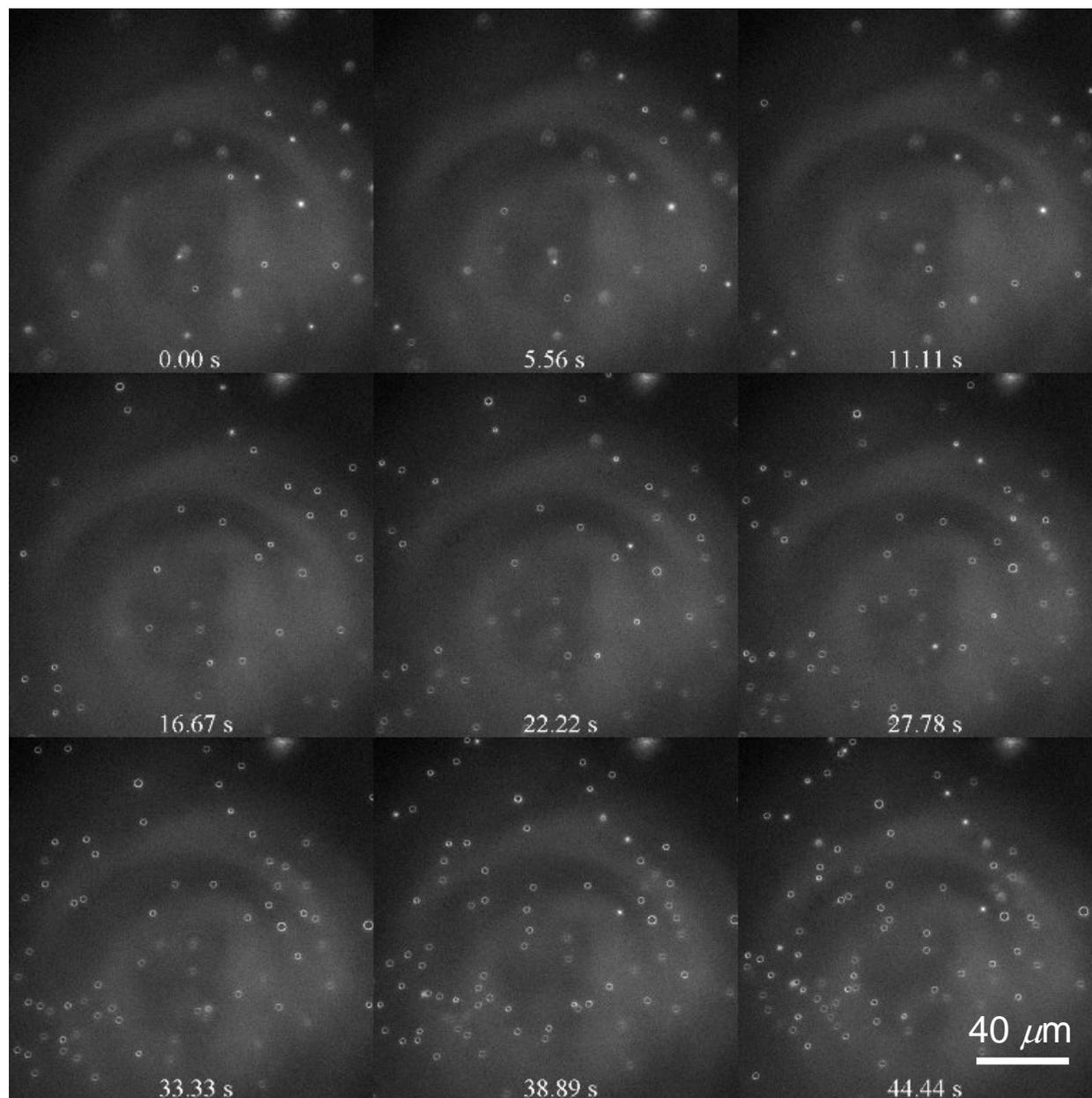
SI Figure 1. Optical image montage for particles during acoustic excitation with 0.5V drive amplitude, revealing limited self assembly at such low powers.
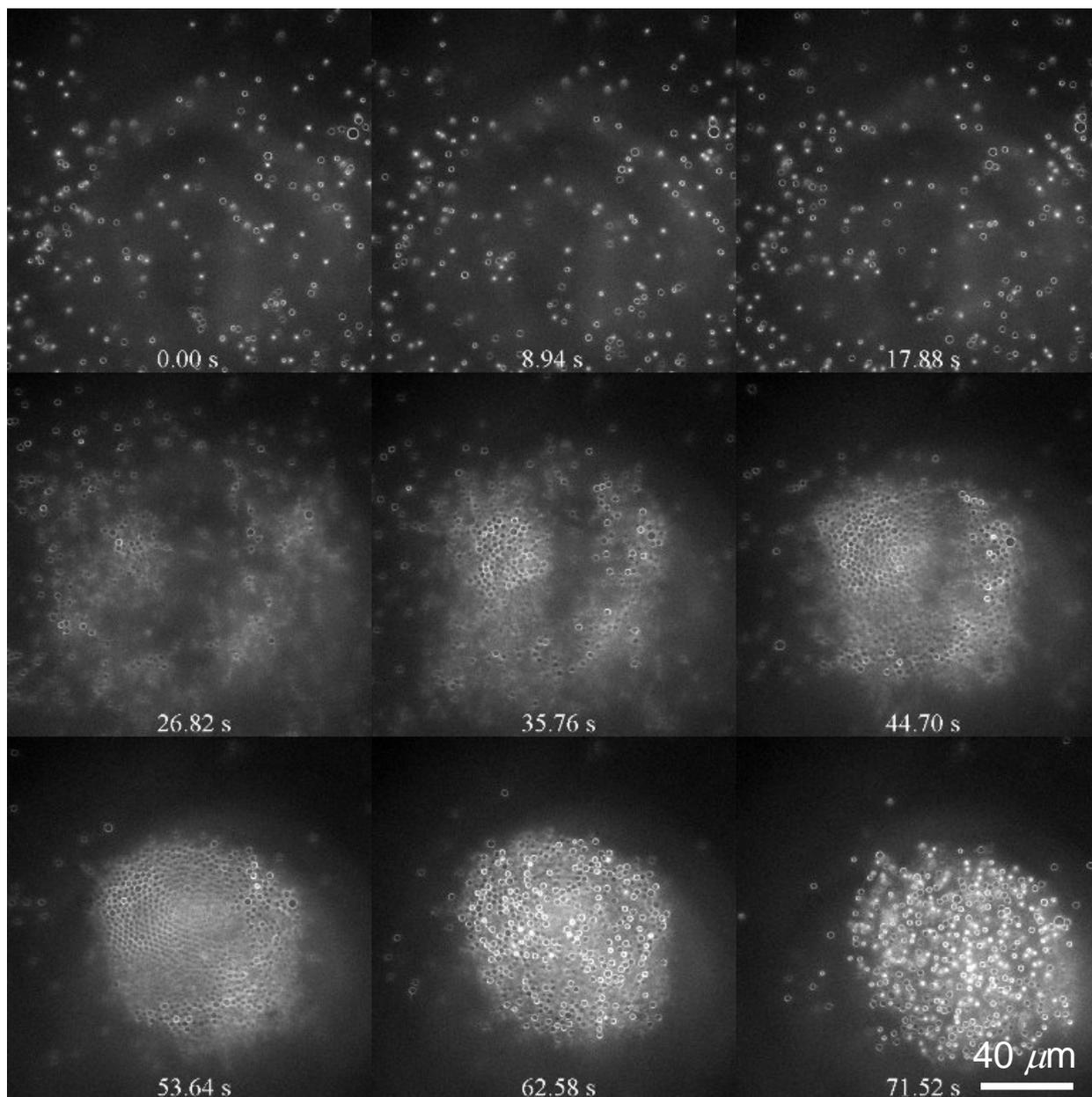
SI Figure 2. Optical image montage for microparticles during acoustic excitation with 1.0V drive amplitude, revealing self assembly at the acoustic focal point. Disassembly via Brownian motion occurs beyond 53.64 seconds (lower left frame) when the acoustic excitation is completed.
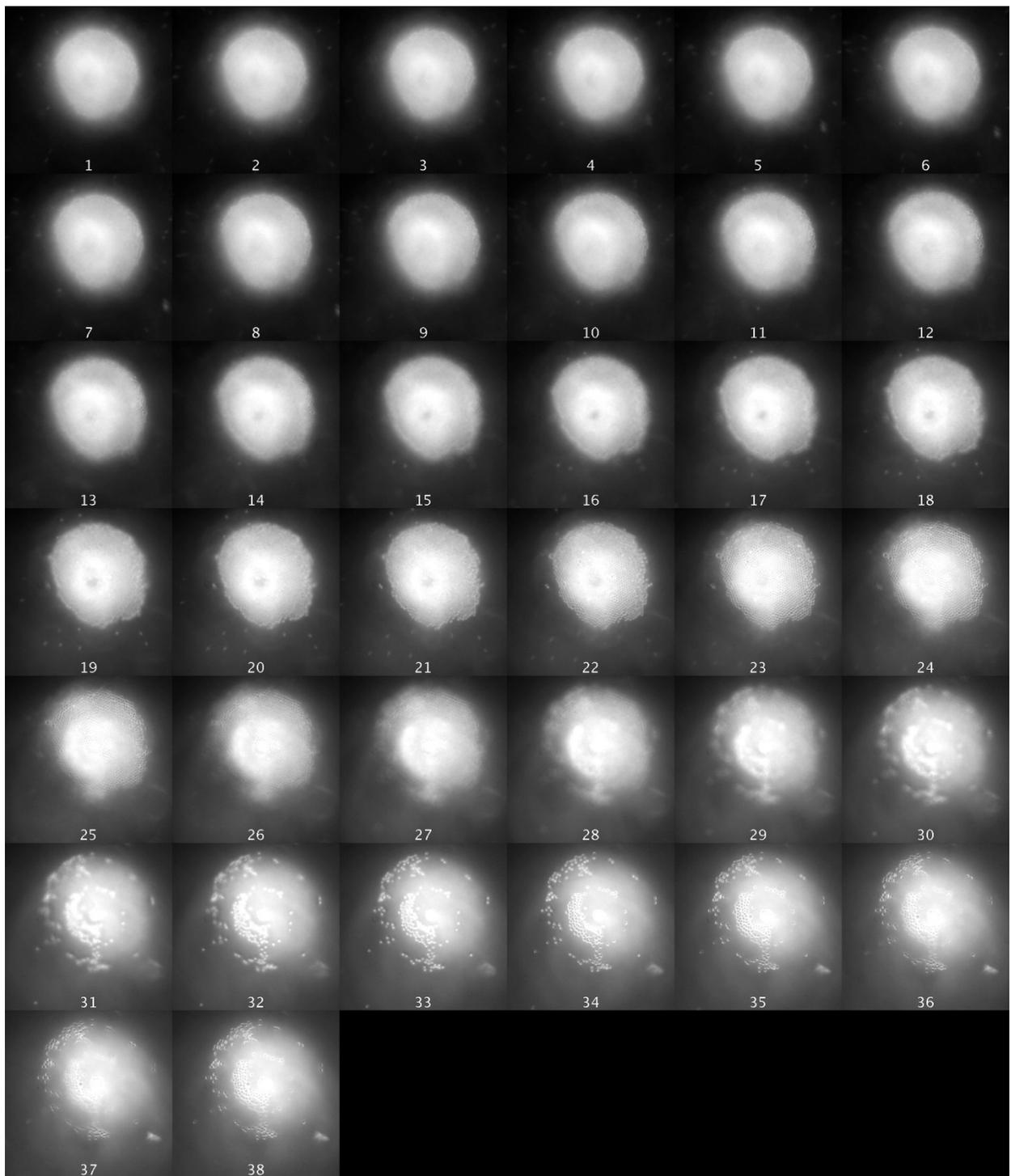
SI Figure 3. Optical z-stack during 1.5 V drive amplitude through a two-layer self-assembly of microparticles.
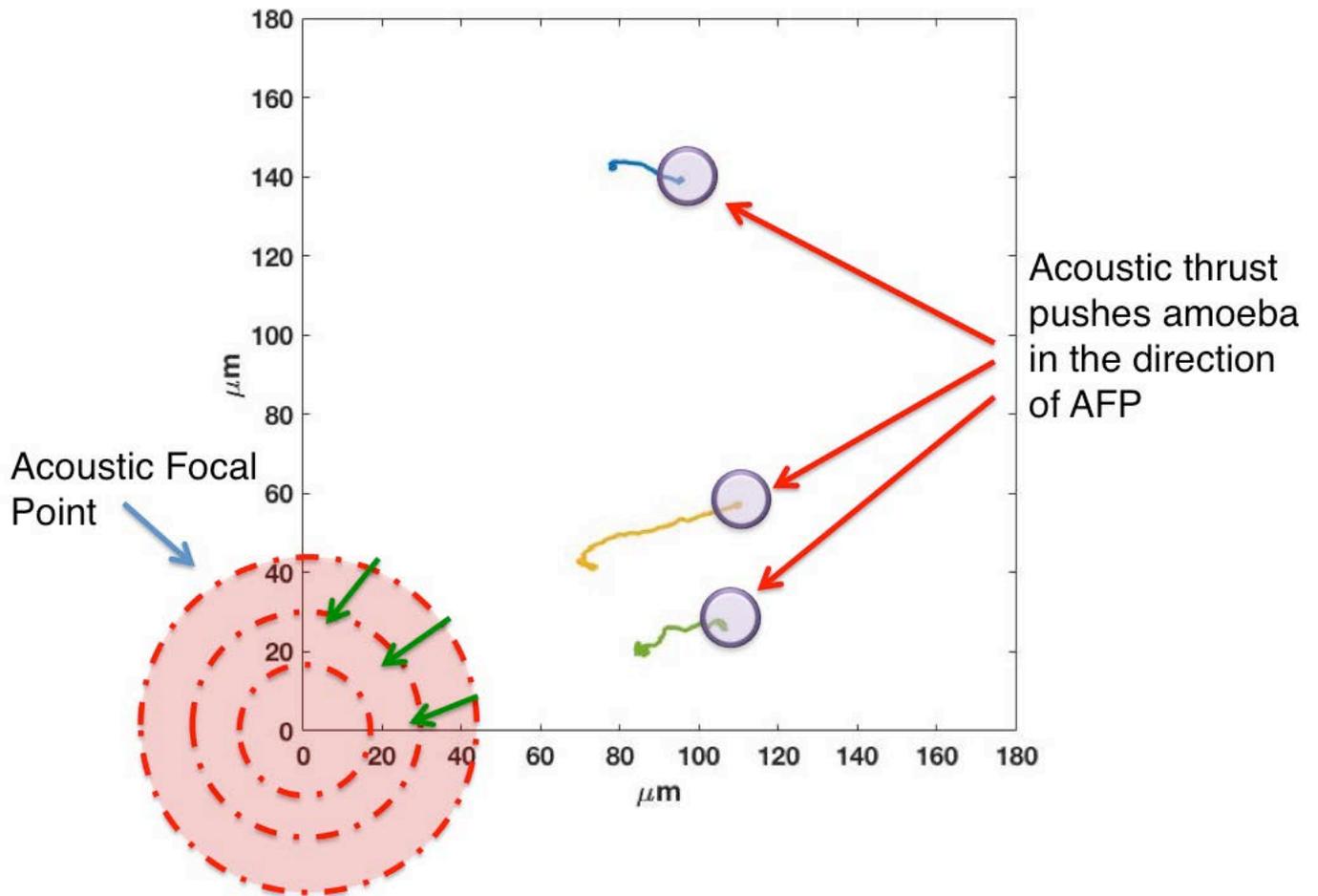
SI Figure 4. Tracks of three distinct amoebas during continuous acoustic excitation with a drive amplitude of 2 V. The acoustic focal point and vectors towards its center are overlain to guide the eye. Two of the amoebas move towards the focal point while the third does not due to other impeding amoeba's (not shown for clarity).